U.S. DEPARTMENT OF COMMERCE
NATIONAL OCEANIC AND ATMOSPHERIC ADMINISTRATION
NATIONAL WEATHER SERVICE
SYSTEMS DEVELOPMENT OFFICE
TECHNIQUES DEVELOPMENT LABORATORY

TDL Office Note 75-8

SIMPLE PROPERTIES OF CHAPEAU FUNCTIONS AND THEIR APPLICATION TO THE SOLUTION OF THE ADVECTION EQUATION

Paul E. Long, Jr. and Farnese J. Hicks

October 1975

Simple Properties of Chapeau Functions and Their Application to the Solution of the Advection Equation

by

Paul E. Long, Jr. and Farnese J. Hicks

ABSTRACT. This note is devoted to the derivation and simple application of chapeau functions. The concept of the Galerkin method for the solution of partial differential equations is introduced, a special case of which is the chapeau function technique. Chapeau functions are used for approximating solutions of linear and non-linear advection equations after certain basic relationships are derived.

1. Introduction

Our decision to use an implicit chapeau function technique in the TDL 3-dimensional boundary layer model [1] was based upon the need to integrate the predictive boundary layer equations efficiently and with reasonable accuracy. The use of an implicit finite difference scheme for integrating the vertical turbulent transfer equations was largely forced upon us; explicit schemes which remain stable with large time steps all seem to suffer badly from consistency problems [2]. The need for an implicit scheme in the horizontal portions of the predictive equations is much less crucial than for the vertical, provided we retain our 80 km horizontal mesh spacing. However, since it is very probable that we will begin experimenting with refined meshes and 2-dimensional telescoping grids in the near-future, we decided in favor of the extra numerical stability of an implicit scheme.

Some initial calculations with one of the simplest and best-known of the implicit schemes, the Crank-Nicolson advection scheme, along with other implicit techniques derived from conventional explicit schemes were not encouraging. Although more stable, the implicit schemes had worse phase errors and computational damping than many standard explicit schemes.

The Crank-Nicolson scheme can be improved by replacing the spatial difference derivative, correct to order $\mathcal{O}(\Delta x^2)$[1], by a spatial derivative correct to order $\mathcal{O}(\Delta x^4)$:

$$\frac{Q_j^{n+1} - Q_j^n}{\Delta t} + \frac{U}{2\Delta x}\left(\delta\, Q_j^{n+1} + \delta\, Q_j^n\right) = 0; \quad \mathcal{O}(\Delta x^2) \qquad 1.1$$

1 See Appendix I for definition of symbols.

then the resulting solution is a solution obtained by Galerkin's method. As another example, let us take the simple advection equation

$$\frac{\partial Q}{\partial t} + U\frac{\partial Q}{\partial x} = 0; \quad U = \text{constant} \qquad 2.5$$

and approximate the solution by basis functions $e_i(x)$ and time-varying coefficients $\alpha_i(t)$

$$Q(x,t) = \alpha_i(t)\, e_i(x) \qquad 2.6$$

The Galerkin method demands,

$$\frac{d\alpha_i(t)}{dt} \int dx\, \dot{e}_i(x) e_j(x) + \alpha_i(t)\; U \int dx\; e_i^!(x) e_j(x)$$

$$\equiv M_{ji}\, \frac{d\alpha_i(t)}{dt} + UN_{ji}\alpha_i(t) = 0 \qquad 2.7$$

where $M_{ji} = M_{ij} \equiv \int dx\; e_i(x)\; e_j(x)$

and $N_{ji} = N_{ij} = \int dx\; e_i^!(x)\; e_j(x)$

If, as is often the case, the trial functions are orthogonal , then

$$M_{ij} = m_i \delta_{ij} \quad \text{and} \quad \frac{d\alpha_i(t)}{dt} + \frac{N_{ji}\alpha_i(t)}{m_i} = 0. \qquad 2.8$$

Suitable basis functions might include trigonometric functions, Legendre polynomials, etc.

We shall choose instead piecewise continuous "chapeau" functions, so-called because each function looks like a hat [Fig. 1]. The figure shows linear chapeau functions defined by the relations

$$e_j(x) = \frac{x - x_{j-1}}{x_j - x_{j-1}} \qquad x_{j-1} \le x \le x_j$$

$$e_j(x) = \frac{x_{j+1} - x}{x_{j+1} - x_j} \qquad x_j \le x \le x_{j+1} \qquad 2.9$$

$$e_j(x) = 0 \qquad \text{otherwise}$$

Although we shall consider only linear chapeau functions in this note, other basis function which vanish outside the interval $[x_{j-1}, x_{j+1}]$ are possible, also.

To apply the linear functions to the simple advection problem we need only to compute M_{ij} and N_{ij}. Unfortunately, chapeau functions are not orthogonal functions; the scalar products $\int dx e_j(x) e_{j\pm 1}(x)$ do not vanish (no summation over j).

We must compute the scalar products indicated by the following figure.

If the values of $Q(x_j, t = 0)$ are defined only at the mesh points x_j and the initial chapeau function solution collocates with the initial conditions, then the chapeau function equation reduces to the finite difference equation,

$$\frac{1}{6}\left[(Q_{j-1}^{n+1} - Q_{j-1}^{n}) + 4\ (Q_j^{n+1} - Q_j^{n}) + (Q_{j+1}^{n+1} - Q_{j+1}^{n})\right]$$
$$+\frac{R}{2}\left[\mu\ (Q_{j+1}^{n+1}) - Q_{j-1}^{n+1} + (1-\mu)\ (Q_{j+1}^{n} - Q_{j-1}^{n})\right] = 0,$$

where $R = \dfrac{U\Delta t}{\Delta x}$.

3. Properties of the chapeau function equation

To examine the stability of (2.16), we substitute $g^n \exp(i\lambda j\Delta x)$ into (2.16). After simplification the result is

$$g = \frac{1 + 1/2 \cos \lambda\Delta x - 3iR/2\ (1-\mu) \sin \lambda\Delta x}{1 + 1/2 \cos \lambda\Delta x + 3iR\mu/2 \ \sin \lambda\Delta x} \qquad 3.1$$

Here g stands for the amplification factor, λ the wavenumber ($\lambda = 2\pi$/wavelength = $2\pi/L$), $i = \sqrt{-1}$ and R the Courant number.

The special case $\mu = 1/2$ is of particular interest; g may then be written as

$$g = \frac{1 + 1/2 \cos(\lambda\Delta x) - 3iR/4 \sin(\lambda\Delta x)}{1 + 1/2 \cos(\lambda\Delta x) + 3iR/4 \sin(\lambda\Delta x)} \qquad 3.2$$

The crucial factor with respect to computational stability is the magnitude of the complex quantity g. Since the numerator and the denominator are complex conjugates of each other, $g = 1$ for all Δt, Δx, and λ. This means the scheme is neutrally stable; there is neither amplification nor damping waves. Choosing $\mu < 1/2$ can lead to computationally unstable schemes (solutions amplified). Setting $\mu > 1/2$ always gives stable scheme with heavy damping.

Since the numerator and denominator of (3.2) are of the form $(a - bi)$ and $(a + bi)$ respectively, g may be written as

$$g = e^{-2i\phi}$$

where ϕ is the real angle

$$\phi = \arctan\left[\frac{3/4\ R \sin(\lambda\Delta x)}{(1 + 1/2 \cos\ (\lambda\Delta x))}\right]$$

The phase speed, c, of (3.2) can be computed from

$$C = \frac{\Theta}{\lambda\Delta t} \quad ; \quad g = |g|\ e^{i\Theta} .$$

The general scheme then reduces to

$$\frac{d}{dt}\left(\alpha_{k-1} + 4\alpha_k + \alpha_{k+1}\right) + \frac{1}{\Delta x}\left[(2\beta_k + \beta_{k+1})\,\alpha_{k+1} - (\beta_{k+1} - \beta_{k-1})\alpha_k - (2\beta_k + \beta_{k-1})\alpha_{k-1}\right] = g_{k-1} + 4g_k + g_{k+1} \qquad 4.6$$

5. Unequally Spaced Mesh Points

One of the features of the chapeau function scheme is the ease by which it can be extended to unequally spaced grid points. Using the irregularly spaced array

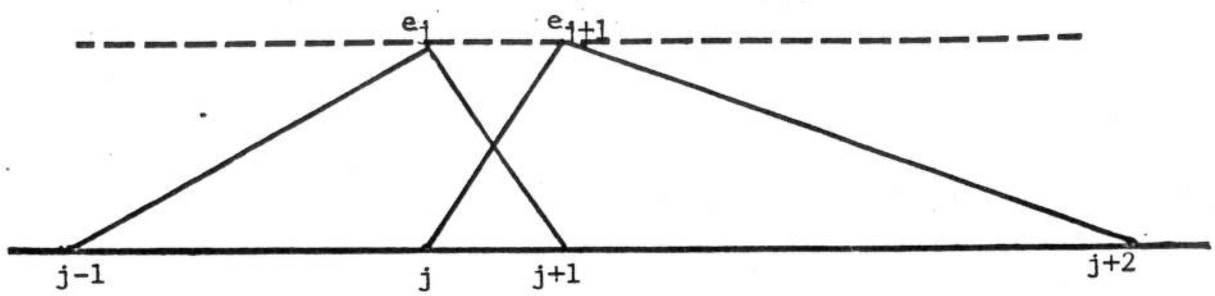

and the notation $h_j = x_{j+1} - x_j$, the new inner product (perhaps "tri-orthogonality" relation would be an appropriate term) becomes,

$$\int dx e_i(x)\, e_j(x) = \frac{1}{6}\left[h_{j-1}\delta_{i,j-1} + 2\,(h_j + h_{j-1})\,\delta_{i,j} + h_j\,\delta_{i,j+1}\right]. \qquad 5.1$$

It can be shown that the advective terms for both the simple linear and general case remain completely unaffected by the variable grid spacing. For the simple linear case,

$$\frac{h_{j-1}}{6}\,Q_{j-1} + \frac{(h_j + h_{j-1})}{3}\,Q_j + \frac{h_{j+1}}{6}\,Q_{j+1} + \frac{U}{2}\,(Q_{j+1} - Q_{j-1}) = 0. \qquad 5.2$$

Variable grids are not without their problems. If a grid is divided into a fine-mesh and coarse-mesh region there will be reflections at the interface whenever a wave passes from one region to the other. We will show an example of this difficulty later.

7. Numerical Examples

A series of 1-dimensional examples is given in [3] along with a fairly lengthly discussion. We will give only the highlights.

In each case, linear and non-linear, the initial state is a Gaussian with a 1/e half-width of two grid intervals centered at $x = 10\Delta x$. The Gaussians ideally should advect at one grid interval per unit time for thirty time units.

Figures 3 and 4 compare the solutions of the chapeau and second-order Crank-Nicolson schemes for increasing Courant numbers ($R = U\Delta t/\Delta x$). Although for large Courant numbers ($R > 2.0$), the two schemes give nearly the same results, the superiority of the chapeau function scheme for smaller Courant numbers is evident. The reduction in the amplitudes comes about by the same mechanism as the creation of the wakes behind the Gaussian: the lagging phase velocity. There is now damping. Figure 5 shows that the solution for the non-linear case is distinguished from the linear case largely by the absence of the wake. This may be caused by the small local Courant numbers except near the center of the Gaussian.

The solution for the 2-dimensional linear case is discussed in the next section. We use Marchuk's concept of "splitting" to solve the 2-dimensional problem [5]. The idea is to solve the x and y direction

$$
\begin{aligned}
T_x \frac{(Q^{n+1/2} - Q^n)}{\Delta t} + \frac{L_x}{2} (Q^{n+1/2} + Q^n) &= 0 \\
T_y \frac{(Q^{n+1} - Q^{n+1/2})}{\Delta t} + \frac{L_y}{2} (Q^{n+1} + Q^{n+1/2}) &= 0 \\
T_x Q_{i,j} &= 1/6 \, (Q_{i+1,j} + 4Q_{i,j} + Q_{i-1,j}) \\
L_x Q^n_{i,j} &= U/2\Delta x \, (Q^n_{i+1,j} - Q^n_{i-1,j}).
\end{aligned}
\qquad 7.1
$$

Here, T is the spatial averaging operator. L is the spatial differencing operator.

8. Boundary Conditions and "Ghosts"

When we used cubic splines [3], pseudo spectral techniques and chapeau functions for the solution of the linear advection equation on a limited area grid with fixed boundaries, we observed a remarkable phenomenon. When an object passed out from the forecast domain, a small amount of noise was generated at the outflow boundary. This noise quickly propagated upstream and collected at the fixed inflow boundary. The amassing of noise at the inflow region is caused by noise which moves rapidly against the flow but can move downstream only at about the same rate as the fluid. In each case, the noise regenerated either a fairly faithful reproduction (a "ghost") of the original Gaussian or gave its mirror (negative) image. With the cubic splines applied to a 2-dimensional limited area grid, the "ghost" was an non-linear advection equation passes from the CM region into the RM region and back into CM. Waves are reflected at both interfaces but particularly at the RM-CM boundary. Figures 9 and 10 show the possible utility of gradually reducing the mesh ratio; the ratio is changed from 4:1 to 4:2:1. This gradual reduction in the mesh ratio resulted in an apparent reduction of the wave reflections at the RM-MRM (moderately refined mesh) interface and at the MRM-CM interfaces.

9. Summary

Chapeau functions are used in the TDL boundary layer model to integrate the horizontal portions of the predictive equations for temperature, wind, and humidity. Chapeau functions, a special case of the Galerkin method, permit the use of longer time steps than would be allowed by usual explicit techniques. For the case of constant 1-dimensional advection, chapeau functions exhibit fourth-order spatial accuracy, can be made absolutely stable and are non-dissipative.

The extension to a 2 or 3-dimensional grid can be carried out by using Marchuk's "splitting" technique.

Fixed outflow boundary values may create "ghosts" at the inflow boundary. The diffuculty may be alleviated by using an implicit upstream differencing scheme at the outflow boundary.

Telescoping grids create related problems. The interface between a refined-mesh and a coarse-mesh region seems particularly prone to reflection difficulties.

10. References

1. Shaffer, W. A., and P. E. Long, 1975: A predictive boundary layer model. NOAA Tech. Memo. TDL-57, 41 pp.

2. Long, P. E., 1975: Dissipation, dispersion and difference schemes. NOAA Tech. Memo. TDL-55, 33 pp.

3. Long, P. W., and W. A. Shaffer, 1975: Some physical and numerical aspects of boundary layer modeling. NOAA Tech. Memo. TDL-56, 37 pp.

4. Finlayson, B. A., 1972: The method of weighted residuals and variational principles. Mathematics in Science and Engineering, Vol. 87, Academic Press, New York, 412 pp.

5. Yanenko, N. A., 1971: The method of fractional steps. Heidelberg, Springer-Verlag, 160 pp.

T	Spatial averaging operator
u	Horizontal wind speed in non-linear problems
U	Horizontal wind speed for linear cases
V	Wind vector
α_i	Time-dependent chapeau function coefficient for scalar variable Q
β_j	Time-dependent chapeau function coefficient for variable advective velocity
Δx, Δt	Finite difference time and space increments
$\doteq$	Approximate equality
$\equiv$	Equivalent to
δ	Central difference operator
$\delta_{i,j}$	Kronnecker delta; $S_{i,j} \begin{cases} 0, i \neq j \\ 1, i=j \end{cases}$
λ	Wave number
μ	Weighting factor
ϕ	Represents $\tan^{-1}(\frac{y}{x})$ where y is imaginary part and x real part of a complex variable

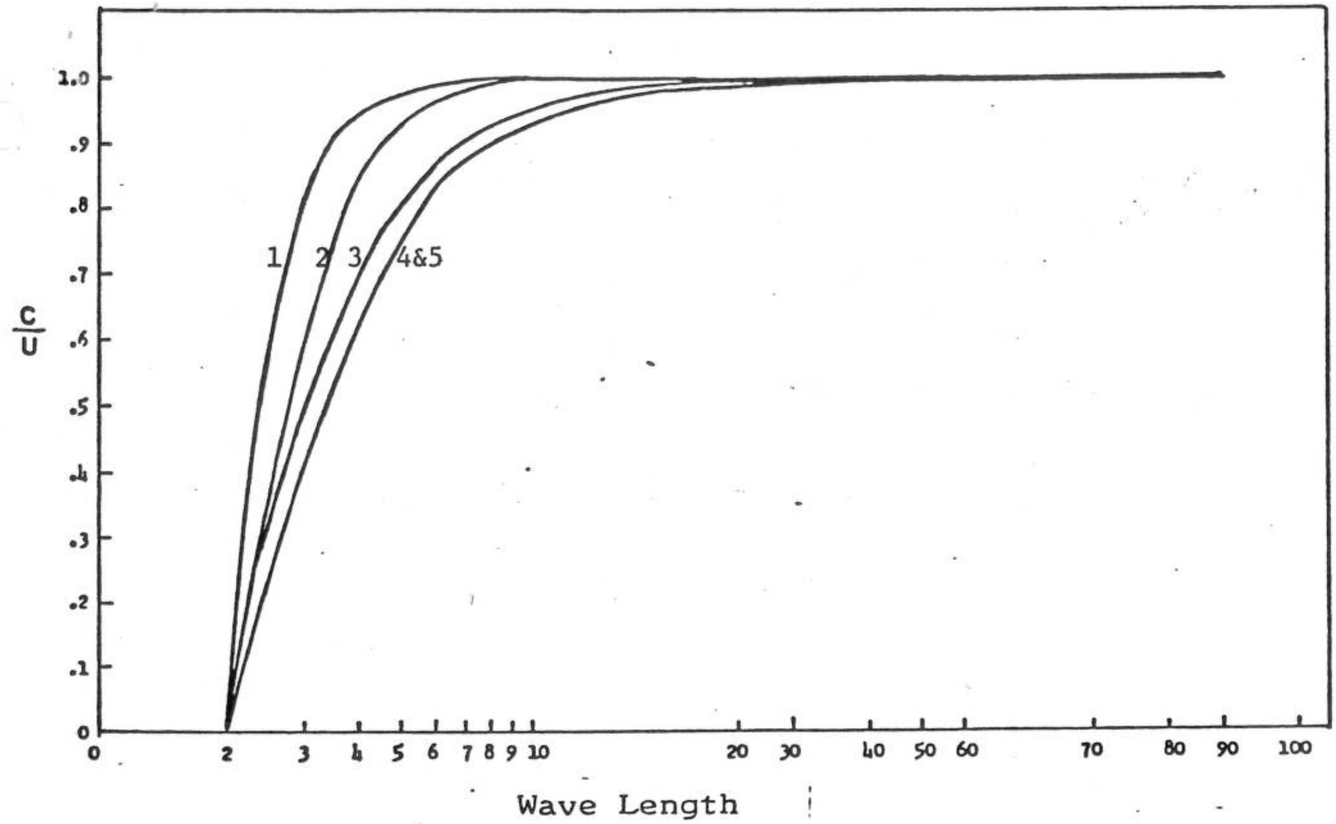

1. **Chapeau Function**

$$1/6\,[(Q^{n+1}_{j-1} - Q^n_{j-1}) + 4(Q^{n+1}_j - Q^n_j)\quad(Q^{n+1}_{j+1} - Q^n_{j+1})] + R/2\,[\mu(Q^{n+1}_{j+1} - Q^{n+1}_{j-1}) + (1-\mu)\,(Q^n_{j+1} - Q^n_{j-1})] = 0, \quad \mu = 1/2$$

2. **4th Order Crank-Nicolson**

$$\frac{Q^{n+1} - Q^n}{\Delta t} + \frac{U}{2\Delta X}\,(Dx\,Q^{n+1}_j + Dx\,Q_j) = 0 \quad \text{where } DxQ_j = 2/3\,(Q_{j+1} - Q_{j-1}) - 1/2\,(Q_{j+2} - Q_{j-2})$$

3. **Upstream**

$$\frac{Q^{n+1} - Q^n}{\Delta t} \quad \frac{U}{\Delta X}\,[\mu(Q^{n+1}_j + Q^{n+1}_{j-1}) + (1-\mu)\,(Q^n_j - Q^n_{j-1})] = 0, \quad \mu = 0$$

4. **Leap-frog**

$$\frac{Q^{n+1}_j - Q^{n-1}_j}{2\Delta t} + \frac{U}{2\Delta X}\,[\,(Q^n_{j+1} - Q^n_{j-1})]$$

5. **2nd Order Crank-Nicolson**

$$\frac{Q^{n+1}_j - Q^n_j}{\Delta t} + \frac{U}{2\Delta X}\,[\mu(Q^{n+1}_{j+1} - Q^{n+1}_{j-1}) + (1-\mu)\,(Q^n_{j+1} - Q^n_{j-1})] = 0, \quad \mu = 1/2$$

Fig. 2. Phase velocities as a function of wavelength for finite difference schemes listed above.

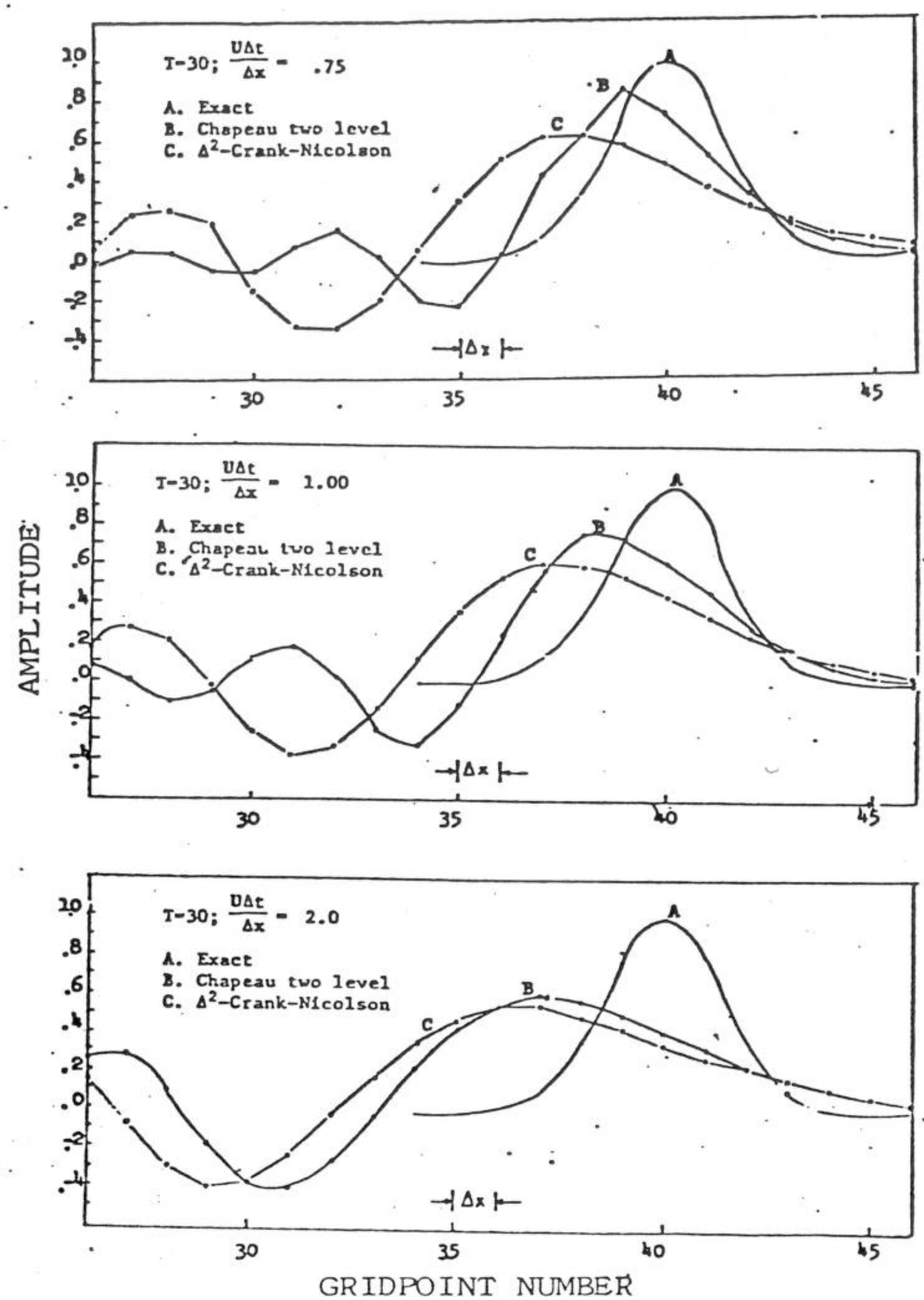

Fig. 4. Extension of Fig. 3 for larger timesteps.

4

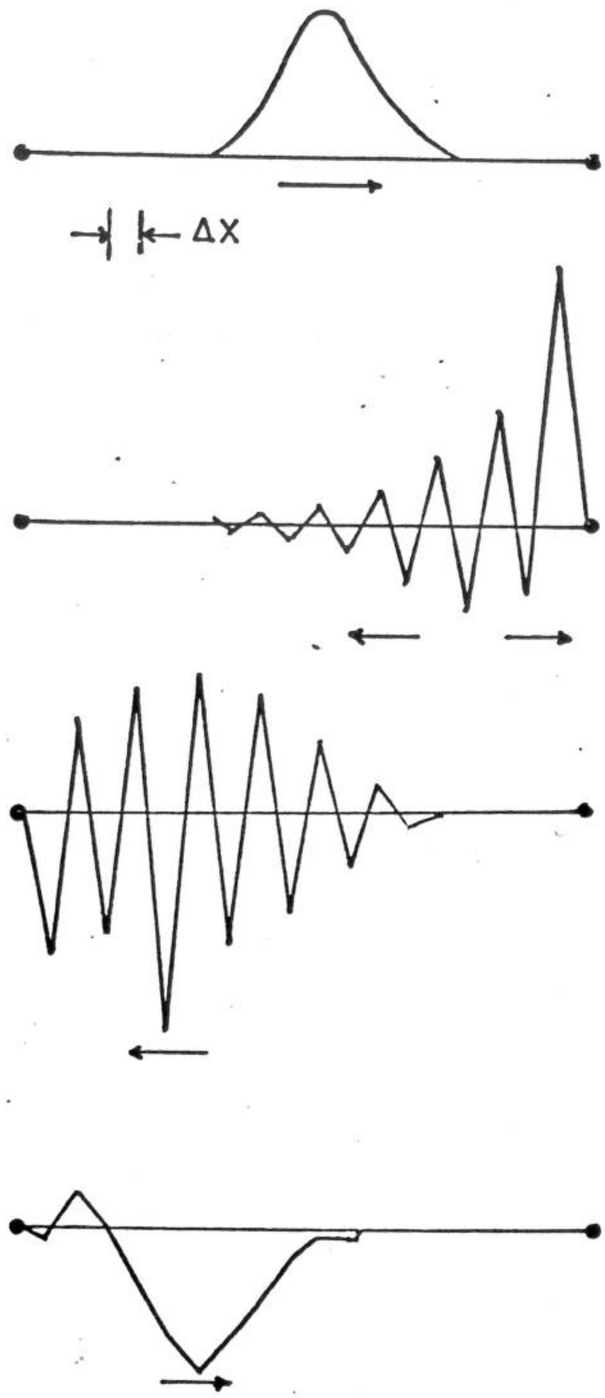

Fig. 6. Conjuration of a "ghost" using a fixed outflow boundary value. Outflow and inflow points are denoted by (•).

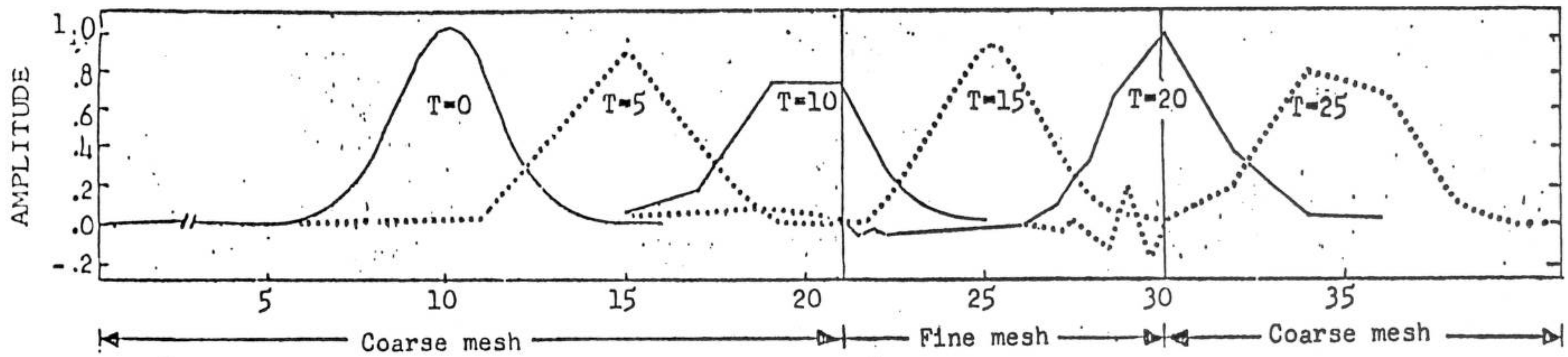

Fig. 8. Evolution of a Gaussian solution to the non-linear advection equation, $\frac{\partial Q}{\partial t} + u(x,t)\frac{\partial Q}{\partial x} = g(x,t)$. Here, once again, chapeau functions advect the Gaussian. Note that the Gaussian passes from coarse mesh (x = 21) and back into the coarse mesh at x = 30, small amplitude waves are generated.

$\Delta t = 0.1$; $(\Delta x)_{coarse} = 2$; $(\Delta x)_{fine} = .5$; Max u = 1.

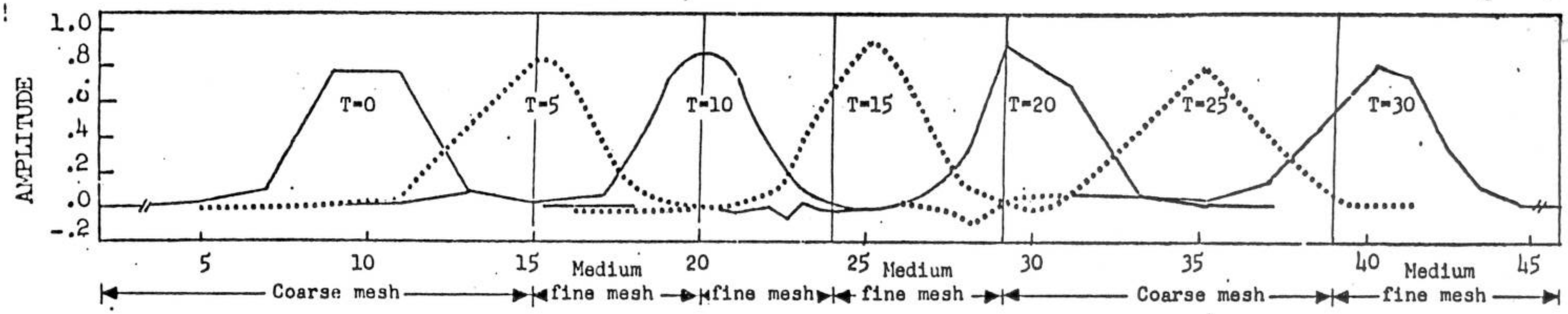

Fig. 10 Similar to figure 9. A Gaussian is advected from a CM region through a MRM region to RM region to MRM to CM to MRM region. Chapeau functions are used to advect the object.

$\Delta t = 0.1$; $(\Delta x)_{CM} = 2.$; $(\Delta x)_{MRM} = 1.$; $(\Delta x)_{RM} = 1/2$; Max $u = 1.$